(NASA-TM-X-73684) STATISTICS OF THE RADIATED FIELD OF A SPACE-TO-EARTH MICROWAVE POWER TRANSFER SYSTEM (NASA) 39 p HC A02/MF A01 CSCL 20N

N77-30314

Unclas
G3/32 42002

NASA TECHNICAL MEMORANDUM

NASA TM X-73684

NASA TM X-73684

STATISTICS OF THE RADIATED FIELD OF A SPACE-TO-EARTH MICROWAVE POWER TRANSFER SYSTEM

by Grady H. Stevens and Gary Leininger
Lewis Research Center
Cleveland, Ohio 44135

1. Report No.	2. Government Accession No.	3. Recipient's Catalog No.
NASA TM X-73684		

4. Title and Subtitle	5. Report Date
STATISTICS OF THE RADIATED FIELD OF A SPACE-TO-EARTH MICROWAVE POWER TRANSFER SYSTEM	6. Performing Organization Code

7. Author(s)	8. Performing Organization Report No.
Grady H. Stevens, Lewis Research Center, Cleveland, Ohio; and Gary Leininger, University of Toledo, Toledo, Ohio	E-9217
	10. Work Unit No.

9. Performing Organization Name and Address	11. Contract or Grant No.
National Aeronautics and Space Administration Lewis Research Center Cleveland, Ohio 44135	
	13. Type of Report and Period Covered Technical Memorandum
12. Sponsoring Agency Name and Address National Aeronautics and Space Administration Washington, D.C. 20546	14. Sponsoring Agency Code

15. Supplementary Notes

16. Abstract

Statistics such as average power density pattern, variance of the power density pattern and variance of the beam pointing error are related to hardware parameters such as transmitter rms phase error and rms amplitude error. Also a limitation on spectral width of the phase reference for phase control was established. A 1 km diameter transmitter appears feasible provided the total rms insertion phase errors of the phase control modules does not exceed 10^{o}, amplitude errors do not exceed 10% rms, and the phase reference spectral width does not exceed ~3 kHz. With these conditions the expected radiation pattern is virtually the same as the error free pattern and the rms beam pointing error would be insignificant (~10 meters).

17. Key Words (Suggested by Author(s))	18. Distribution Statement
Power transfer Microwaves Phase control	Unclassified - unlimited STAR Category 32

19. Security Classif. (of this report)	20. Security Classif. (of this page)	21. No. of Pages	22. Price*
Unclassified	Unclassified		

* For sale by the National Technical Information Service, Springfield, Virginia 22161

SUMMARY

Statistics such as average power density pattern, variance of the power density pattern and variance of the beam pointing error are developed for a 1 km diameter monolithic transmitter and related to subsystem hardware parameters such as rms phase insertion error and rms RF power level error. Also a limitation was established on the spectral width of the phase reference used in the phase control subsystem. A 1 km transmitter in space appears technically feasible with performance virtually the same as an ideal antenna providing: (1) the total rms phase error on the transmitter does not exceed 10^{0}, (2) the rms amplitude error on the transmitter does not exceed 10%, (3) the spectral width of the phase reference does not exceed $\sim$3 kHz. Given such conditions the first sidelobe level would be within 1.5 db of the error free case with 99.99% confidence. Also, the maximum pointing error would be less than 37 meters with 99.99% confidence.

INTRODUCTION

It has been demonstrated that microwaves can be an efficient medium for power transfer (reference 1,2). Tests at Raytheon (Waltham, Massachusetts) have demonstrated a short range DC-DC link efficiency of 54 percent while recovering 495 watts of DC power (reference 1). A recent test at the NASA-JPL complex at Goldstone, California demonstrated long range (1.54 km) transfer of power with recovery of 30.4 kw of DC (reference 2).

These small scale tests were intended to make preliminary evaluations of the feasibility of long range power transfer with microwaves on a large scale. One application of this technique would be the collection and conversion of solar energy in geosynchronous orbit and transmission of this energy to earth via microwave link as in the Satellite Solar Power Station (SSPS) concept (reference 3). There are possible terrestrial applications as well including underground waveguide links (reference 4). In addition there has been proposed an application involving a geosynchronous reflector for point-to-point relaying of power on earth (reference 5).

The SSPS concept was originated by Dr. Peter Glaser of A.D. Little, Inc. This concept makes use of photovoltaic converters for solar-DC conversion and high efficiency cross field amplifiers (amplitrons) for DC-RF conversion. A feasibility study of this concept was published as NASA CR-2357 (reference 3).

Subsequent studies (references 6-9) addressed the detailed requirements of the microwave power transmission system (MPTS). In particular, a Raytheon study (references 6-8) provided an assessment of critical technology areas, impact of uncertainties on system cost, preliminary assessment of environmental impact, as well as RFI impact. Also included was a suggested plan for development and verification of critical technologies and techniques.

Another study (reference 9) addressed similar questions but also included a preliminary assessment of the economic impact of possible environmental and hardware constraints.

In the course of these studies it became apparent that very large antennas would be required for power transfer from space-to-earth. The need for the receiver to fill the main lobe of the transmitter at a distance of 23,000 km led to the selection of an approximately 1 km diameter transmitter and 10 km diameter receiver at 2.45 GHz. In principle frequencies above 2.45 GHz would tend to reduce the required antenna sizes. However, other constraints such as transmitter structural thermal limitations and peak receiver RF power density restrictions place a minimum size limitation on the transmitter and receiver and as a consequence there is little frequency advantage above 2.5 GHz. In addition rain losses as well as subsystem inefficiencies are of sufficient significance above 2.5 GHz as to actually cause system cost ($/delivered kw) to rise above 2.5 GHz. As a result, 2.45 GHz would be an effective transmission frequency, being in the appropriate

range from a cost viewpoint as well as having minimal spectral impact (lies in the industrial microwave band) and yielding a feasible system with respect to potential constraints.

To efficiently concentrate the transmitted power in the main lobe of such a system, it is necessary to maintain very precise amplitude and phase distributions over the transmitter aperture. Static phase and amplitude errors not only degrade transmission efficiency, they also raise the sidelobe level and cause pointing errors of the maintain lobe. With a system such as this, which typically would operate in the 5 GW range, the uncertainty in beam pointing and sidelobe levels can be critical. Therefore it is appropriate to assess the expected degradation in efficiency, the likelihood of the sidelobes exceeding some predetermined level and the expected pointing error.

The purpose of this paper is to present preliminary estimates of these parameters and relate them to the technical requirements of the system.

SYSTEM CONCEPT

A typical geometry for a space-to-earth microwave power transmission system is shown in Figure 1. As was shown in other studies (references 3,6-9), the required transmitter diameter is nominally 1 km and the receiver, nominally 10 km, is sized to intercept 90 percent of the main lobe. More interception can be realized by increasing the transmitter or receiver diameter but cost analyses have shown (references 6-9) a diminishing return above 90-95 percent interception.

Typically the transmitter might be a planar array segmented into many small arrays of the order of 20 meters on a side. Each of these smaller arrays might be attached to a monolithic support structure having means for independent pointing and positioning.

This concept is a consequence of relaxing the mechanical rigidity requirements in the interest of reducing on-orbit weight of the transmitter.

As a consequence, gravity gradient perturbations, variations in solar pressure, periodic thrusting for attitude control, and thermal cycling will perturb the structure. Without compensation the resulting deformations would be of sufficient significance to degrade the transmission efficiency and pointing to an intolerable level. To compensate for these deformations and maintain efficiency as well as precise pointing, it has been proposed that a retro-directive phase control approach (references 3.6-9) be used.

Such techniques have been demonstrated (references 10-12) on a small scale and shown to operate successfully. A very simplified schematic of a typical system is illustrated in Figure 2. The transmitter is illustrated in this system, as a one dimensional linear array of special conjugation modules and the receiver is illustrated as having a centrally located transmitter which emits a stable reference signal in the direction of the orbiting transmitter. Since each receive/transmit module lies at a different distance from the ground receiver the locally sampled signal at each of the orbiting modules bears a different phase relation with the ground reference.

In this simplified system each module routes this received signal to a special processor which performs a conjugation. The conjugated signal is then routed back to the antenna, amplified, and retransmitted. Note the argument of the transmission for each orbiting module corresponds exactly to the path delay for that particular module but reversed in sign. If the attitude of the transmitter were perfectly stable, the transmission would experience an identical path delay on the downlink, arriving in phase with the ground reference. Since this would be true for each of the modules all the transmissions will be in phase at the receiver. Note this is true no matter what the orientation of the power transmitter even for relative displacements of the conjugation modules. Hence, in this simplified case, this technique can provide automatic steering of the beam, automatic focusing of the beam, (a necessity in the fresnel zone) and compensation for deformation of the transmitter structure.

Several techniques have been used to perform the conjugation (references 10-12) and a heterodyning method is illustrated in Figure 3. For simplicity assume a reference plane has been established by using the signal received by one of the orbiting conjugation modules as a phase reference. This signal, Wo, would be distributed to each of the remaining modules where it would be heterodyned with a locally generated signal, W_{IF} (bottom of Figure 3). Two sidetones are produced, $Wo \pm W_{IF}$, which are separated by filters and distributed to two other mixers. The upper sidetone, $Wo + W_{IF}$, is heterodyned with a local sample of the uplinked reference frequency, Wo. This module is shown displaced with respect to the reference module and it will therefore see the reference frequency as having a different phase, related to the amount of displacement, given by

$$\phi = \frac{2\pi \Delta X}{\lambda} \qquad (1)$$

where $-\phi$ is the apparent phase of the locally received signal relative to that received by the reference module. ΔX is the relative displacement of the local module and λ is the wavelength of the reference frequency, Wo. The displacement could be the result of a deformed or perturbed antenna surface.

After heterodyning with the locally received signal, a lower sidetone, having the same frequency and phase as the locally generated signal W_{IF}, is separated by a bandpass filter and routed to an output mixer. Note the phase displacement, ϕ, is preserved but reversed in sign. A second heterodyning in the output mixer produces a sidetone having the same frequency as the reference, Wo, but having a relative phase identical to the conjugated phase displacement, $+\phi$.

Since the processing is so rapid the local module motion would be insignificant during this interval and would have the same relative position with respect to the reference module upon retransmission. Consequently the path delay with respect to the reference plane will be the same as that experienced by the received signal. Since the conjugation process provides an initial phase delay equal and opposite in sign to that on receive, the retransmitted signal will arrive at the reference plane in phase with that signal retransmitted by the reference module. Therefore all modules will operate in concert regenerating a constant phase contour which duplicates the phase contour of the incoming reference signal. Therefore, an incident plane wave will be re-radiated as a plane wave and in the direction from whence it came. Furthermore an incident spherical wave will be retransmitted as a spherical wave with reversed curvature so that the transmitted beam is steered onto and focused upon the ground receiver. Ideally, the system would operate as described providing the self-focusing, self-pointing features previously described. In reality, there are complications which, if not accounted for and controlled, could cause significant degradation of system efficiency.

For example, in a real system, the spaceborne transmitter could have sufficient motion as to cause measurable doppler shift of the uplinked reference frequency. This would be most significant when the transmitter is being slewed through a limit cycle with respect to the ground receiver or when the transmitter structure responds to an attitude change. In these cases the orbiting reference module will not see the same doppler shift as the other modules and all transmissions would be

at slightly different frequencies. It is not clear at this time, if this effect could seriously affect beam efficiency. Preliminary attempts at modeling this effect have led to completely opposite results. One model indicates that, in the presence of doppler shift, the separation between the receiver and transmitter must be accounted for and leads to unacceptable beam degradation or severe restrictions on structural motion. An alternate model indicates that only the motion relative to the reference conjugation module needs to be accounted for and leads to virtually no beam degradation and liberal restrictions on structural motion. Continuing studies on this subject are being pursued by others.

Another potential problem is the need for isolation of the uplinked referenced signal and the downlinked power beam. It appears sufficient isolation can be achieved by such methods as polarization discrimination and/or the use of affect pilot tones and frequency discrimination. However, this should be verified experimentally.

In addition there will be a need for compensating the non-zero phase insertions of components and subsystems. In particular the distribution of the centrally received reference frequency, Wo, to each of the conjugation modules is critical. It is easily shown that any phase error introduced during reference frequency insertion at the local modules appears in the output of those modules with its magnitude doubled. Fortunately, reference frequency distribution has successfully been accomplished over large apertures in systems designed for radio astronomy. In particular it has been demonstrated (reference 13) that reference distribution can be accomplished with coaxial cables having electronic

path length compensation. The method has similarities to the aforementioned retro-directive approach with the transmission medium being the coaxial cable. Phase errors were held to within 1^{o} rms over a 600 meter baseline by this method. Similar methods have been proposed for reference distribution in the Cyclops concept (reference 14).

One such method (reference 14) is illustrated in Figure 4. On the right side of the figure is shown a voltage controlled oscillator which, without control, would operate at a frequency $\frac{Wo}{2} + \delta$ and have a phase offset ϕ.

The output of this oscillator is transmitted via coaxial cable to a reference module which provides the reference frequency, Wo. Propagating along the line the VCO signal acquires a phase displacement according to the length of the line, ℓ . The phase displaced VCO signal is then heterodyned with the reference frequency, Wo, at the reference module. The resulting lower sidetone has the same frequency as the VCO signal but has the opposite phase displacement. This lower sidetone is then sent back along the same coax to the originating module. This return signal will experience an almost identical phase displacement on the return path so that when received it has only the phase residuals $2\ k\ \delta\ \ell$ and the VCO phase offset ϕ. An additional heterodyning results in an upper sidetone with a frequency identical to the reference, Wo, but having a phase residual due to the VCO frequency offset δ . Using the lower sidetone produced in the same operation to control the VCO, a phase locking operation is initiated so that the offset, δ , is identically zero when the loop locks. Thereafter, the regenerated

reference frequency would be error free. In practice the distribution method would be more complicated than this to overcome some of the practical difficulties in the above technique. For example, when the system is locked each module is required to separate incoming and outgoing signals which have the same frequency but possible much different power levels. This is not easily done and variations on the above method are used so that incoming and outgoing signals are at different frequencies (references 13,14). As a consequence, Figure 4 is not exactly representative. However, it does illustrate the basic methodology and it provides a means of illustrating possible phase insertions that will not be compensated. In addition to the insertion errors of the filters and mixers there can be significant errors due to imperfections in the coaxial cables. Remember that a multitone reference frequency distribution technique is desirable for isolating incoming and outgoing distribution signals at the receive/transmit modules. Since the phase constant of coaxial lines is typically a function of frequency, the compensation of phase errors by this technique is less than ideal and limited by the required bandwidth of the distribution system and coaxial line quality in terms of dispersion. Fortunately, in power transmission systems, very narrow bandwidths are acceptable and as a result cable dispersion is not expected to cause significant errors.

Another phenomenon of concern is the required coherence of the reference frequency source. As the output of this source is distributed over the transmitter aperture the locally regenerated

reference signals at the transmit/receive modules will have increasingly larger differential time delays with respect to the original reference source. In effect, the modules at the transmitter edges will be excited by a reference frequency which has been time delayed by the radius of the transmitter. This would be of no concern if the VCO frequencies and the reference source were ideal tones. However, these frequencies will have finite spectral widths, and differential time delays in finite spectral width signals cause decorrelating effects which tend to reduce aperture efficiency (reference 15). The amount of decorrelation and consequent loss of aperture efficiency depends on the spectral width of the source, how it is distributed, and the size of aperture. Analyses have shown (reference 15) that an aperture illuminated with a signal having a typical distance L for 63% decorrelation will result in the antenna pattern having a peak power density 20% down from the ideal if the transmitter radius is as much as 25% of the distance L . For smaller radius/L ratios this relationship is approximately proportional so that for losses to be held less than 1% the transmitter radius should not exceed 1.3% of the decorrelation distance, L.

The decorrelation distance L can be approximated a variety of ways. One simple method is arrived at by assuming the reference frequency source can be modeled as very narrowband noise. Assuming the reference frequency has a spectral power density which is constant over the spectral width Δf and zero outside this width, an autocorrelation of such a signal would have the form,

$$R(\tau) = 2\Delta f \frac{\sin(2\pi\Delta f \tau)}{(2\pi\Delta f \tau)} \cos(2\pi\Delta f \tau) \qquad (2)$$

which indicates the degree of correlation of the signal with a replica of itself delayed in time by amount τ . The envelope of this function equals 0.37 (63% decorrelation) when the following is satisfied,

$$2\pi \Delta f \tau = 2.194 \qquad (3)$$

This corresponds to a time delay, τ , of

$$\tau = \frac{0.3492}{\Delta f} \qquad (4)$$

This time delay is equivalent to the distance

$$L = C \tau$$

with C being the propagation velocity in the coax cable (approximately 3×10^8 m/s).

As mentioned before, the aperture radius should not exceed 1.3% of this dimension if the aperture efficiency losses due to decorrelation effects are to be held within 1%. For a radius of.500 meters then the reference spectral width should not exceed

$$\Delta f = \frac{(0.013)(0.3492)C}{500} = 2.7 \text{ kHz} \qquad (5)$$

an easily achievable spectral width at 2.45 GHz. Therefore, incoherence effects due to a finite spectral width frequency reference is not expected to be a significant problem.

EFFECTS OF STATIC AMPLITUDE AND PHASE ERRORS

A fundamental equation defining the radiated field produced by a steady state sinusoidal field distribution on a transmitter aperture is given by the approximate relationship:

$$U(X_o,Y_o) = \frac{1}{j\lambda Z} \int_{-\infty}^{\infty}\int_{-\infty}^{\infty} U(X_1, Y_1)\exp\left[-j\frac{2\pi}{Z}(X_oX_1+Y_oY_1)\right] dX_1dY_1 \quad (6)$$

where $U(X_o, Y_o)$ is the field variable at the receiver, $U(X_1,Y_1)$ is the field variable at the transmitter, Z is the separation between the transmitter and receiver, and λ is the wavelength of the exciting field. The approximation is valid even within the Fresnel zone (reference 22) provided,

1) The range on (X_o, Y_o) and (X_1, Y_1) is such that for all values of (X_o, Y_o) and (X_1, Y_1) within this range the distance between (X_o, Y_o) and (X_1, Y_1) is essentially constant and equal to Z.

2) $U(X_1, Y_1)$ is the result of a focusing operation where,
$$U(X_1, Y_1) = U(X_1, Y_1) \cdot \exp\left[-j\frac{\pi}{\lambda Z}(X_1^2 + Y_1^2)\right]$$
is the actual field distribution which includes a quadratic focusing factor. For computational purposes the quadratic focusing factor can be ignored as it has already been accounted for in deriving (6).

This relation can be used to determine the power distribution at the receiver for any arbitrary choice of amplitude and phase distributions at the transmitter. By adding appropriate spatially dependent perturbations on amplitude and phase, the effects of specific errors in amplitude and phase can be determined. And by repeating the process in a Monte Carlo fashion, one can arrive at a statistical description of effects of amplitude and phase errors.

Of interest would be the mean power density on axis at the receiver, the mean sidelobe level, variance of the sidelobe envelope, and variance of the main lobe from its intended direction. All these effects could be determined using the above procedure but extensive computational effort, would be required.

Fortunately, analytical models for these statistics have been developed (references 16-21) which offer straight forward computational alternatives provided one is willing to accept the inaccuracies of attendent approximations. These inaccuracies have been addressed in a qualitative sense by comparison with actual antenna patterns (reference 16) and Monte Carlo simulations (reference 21). These qualitative results indicate the errors involved to be of little significance at this point of the MPTS concept. Accordingly, these models have been appropriately modified where necessary and used to determine estimates of the aforementioned statistics.

Degradation of the Main Lobe and Sidelobe Envelope

If one were to imagine that a particular transmitter, having a particular amplitude and phase distribution, was one of many that could have been constructed, then the expected power pattern at the receiver could be computed by taking the average of all the possible radiation patterns at the receiver.

Such analyses have been done by others which include both amplitude and phase error effects (references 16-18). The results are directly applicable to the microwave power transmission system in question provided

a small modification is made to account for the unique method of RF power distribution in this system.

The current concept of such a system includes a transmitter having a quantized power distribution established by an array of individually excited 18 meter x 18 meter subarrays. Amplitude and phase variations within a subarray would be so slight as to be of no significance (reference 9). However, the variation from subarray to subarray would be significant. Random error in setting the excitation of each of the subarrays is likely to be uncorrelated (the correlated errors are predictable and could be corrected by the RF power distribution system) which justifies a significant simplification of the required analysis.

Such an analysis is presented in Appendix I which essentially follows the same procedure as described in references 16 and 18. The analysis of Appendix I, however, includes the necessary modification to account for the use of large and directive radiating elements (18m x 18m subarrays) instead of non-directional isotropic radiating elements. One result of this analysis is an expression relating the average power pattern at the receiver to the rms amplitude and phase errors given by,

$$\langle p(x_0,y_0)\rangle = \frac{P_t}{4\pi z^2}\left[G(x_0,y_0)\exp(-\sigma_\phi^2)+(K^2+1-\exp(-\sigma_\phi^2))\,Gsa(x_0,y_0)\right] \quad (7)$$

where,

$G(x_0, y_0)$ is the overall array gain with no phase or amplitude errors (includes quantization effects.)

$Gsa(x_0, y_0)$ subarray gain pattern for uniform power distribution on subarray.

K^2 fractional mean square random amplitude error.

$\sigma\phi^2$ mean square phase error.

P_t ensemble average power in illumination field.

The first term in the brackets of (7) is just the usual power density for an ideal antenna but decremented by an exponential factor related to the variance of the transmitter phase error. The second term also has the form of an antenna pattern but being more extensive in coverage since it is determined by the subarray size. The equivalent power into this second pattern can be interpreted as scattered power being a function of not only the phase error but the mean square amplitude error as well.

In Figure 5 the result of adding two such patterns is shown for the particular case of 10 degrees rms phase error, 10% rms amplitude error, and for 18 x 18 meter subarrays. This also assumes a 1 km transmitter having a particular distribution of power (reference 9) with an edge power density10 db less than the peak power density.

The effect of the scattered power pattern is to fill in the nulls of the coherent pattern and raise the sidelobe level slightly. For example, in the case cited, the main lobe power density would be degraded by 3% and the expected far sidelobe level could be raised as much as 2-3 db. One should keep in mind that this represents only what one should expect on the average. A particular radiation pattern could have significant variation about this mean pattern (references 16, 18).

Therefore, it is of interest to determine the likelihood of a significant departure from this pattern. This is especially true of a microwave power transmission system where power density levels outside the main lobe must be maintained below acceptable exposure levels (reference 9).

To make this determination one needs a statistical description of the variation about the mean pattern obtained above. Analyses have shown (references 18, 20) that the magnitude of the electric field at the receiver has a statistical distribution of the form of a modified Rayleigh or Rician distribution. Making suitable adjustments to make these results directly applicable to the case at hand (Appendix I), the electric field magnitude has a distribution described by

$$W\left[r(x_o, y_o)\right] = \frac{2\, r(x_o, y_o)}{\sigma^2} \exp\left[-\frac{r_o^2(x_o, y_o)+r^2(x_o, y_o)}{\sigma^2}\right] I_o\left(\frac{2r_o r}{\sigma^2}\right) \quad (8)$$

where $r(x_o, y_o)$ is the normalized field strength for the actual system given by

$$\langle r^2(x_o, y_o)\rangle = \frac{4\pi \bar{z}^2 \langle p(x_o, y_o)\rangle \exp(\sigma_\phi^2)}{G(o,o)} \quad (9)$$

$r_o(x_o, y_o)$ is the normalized field strength for an error free system given by

$$r_o^2(x_o, y_o) = \frac{G(x_o, y_o)}{G(o,o)} \quad (10)$$

σ^2 is the normalized field strength variance given by

$$\sigma^2 = \left[1 + K^2 - \exp(\sigma\phi^2)\right] \exp(\sigma\phi^2) \frac{Gsa}{G(o,o)} \quad (11)$$

and I_o is the modified Bessel function of the first kind.

The probability that the normalized sidelobe level, r, does not exceed a specified limit, R, is then given by,

$$P\left[r(x_o, y_o) < R\right] = \int_0^R W\left[r(x_o, y_o)\right] \quad dr \qquad (12)$$

or,

$$P\left[r(x_o, y_o) < R\right] = 1 - \int_R^\infty W(r(x_o, y_o)) \quad dr \qquad (13)$$

The integral in equation (13) has been tabulated and is available from the literature (reference 23). Selecting a particular probability, say 99.99%, equation (13) and available tabulations enable the determination of the corresponding sidelobe level. For example, Figure 6 compares the 99.99% confidence limit with the same expected pattern shown in Figure 5. With only a 10^o rms phase error and 10% rms amplitude error, the 99.99% limit for the first sidelobe is within 1.5 db of that of the average level.

However, the upper confidence limit for the far sidelobes is significantly higher than the average level reflecting the greater variance of the sidelobe level in this region and the greater uncertainty as to what form the sidelobe pattern of a particular system might be.

The maximum sidelobe level is of interest in determining the power density to which a surrounding population might be exposed to on a continual basis. Alternatively, the sidelobe envelope can be used to determine the required diameter of a surrounding restricted region outside of which the continuous exposure level would be below some specified value. As indicated above this specification must be done on a statistical basis. For example, if the peak power density in Figure 6 were 23 mw/cm^2, a restricted region of about 18 km diameter would insure that the population outside this region

would be subjected to no more than 0.1 mw/cm^2 with 99.99% confidence. Higher levels of confidence can be obtained by simply using a larger diameter restricted region or by tighter phase and amplitude control on the transmitter.

Beam Pointing Error Statistics

Using equation (6) the local power density at the receiver is proportional to

$$p(x_o, y_o) = U(x_o, y_o) \cdot U^*(x_o, y_o) \tag{14}$$

Beam direction is defined as the direction of the peak of the power density function in (14). Therefore one could locate the peak or beam direction by solving the equations,

$$\frac{\partial p(x_o,y_o)}{\partial x_o} = 0$$

$$\frac{\partial p(x_o,y_o)}{\partial y_o} = 0 \tag{15}$$

In general this would be a formidable task. However, with the restrictions of small range on (x_o,y_o) about the no error direction and a small rms phase error on the transmitter, Taylor series approximations to the power density in (14) can be used to derive tractable forms of equations (15) (references 19, 20).

One such analysis (reference 20) gives an rms pointing error of the form,

$$\Delta\Theta \text{ rms} = \frac{\sqrt{3}}{\pi} \frac{\lambda\sigma}{dM} \tag{16}$$

Where σ is the rms phase error on the transmitter, d is the center-center spacing of the subarrays, and M is the total number of subarrays. The rms beam displacement at the receiver is then

$$\Delta x_o \text{ rms} = \Delta y_o \text{ rms} = \ell\, \Delta\Theta \text{ rms} \tag{17}$$

where $\bar{z}$ is the distance between the transmitter and receiver. For example, with an rms phase error of 10^{o} on the transmitter, a wavelength of 0.122 meters (2.45 GHz), 18 meter subarrays, and 2400 subarrays (1 km circular transmitter), the rms beam displacement would be about 10 meters. Since the receiver in a microwave power transmission system would be on the order of 8 km in diameter (references 5-8), such a beam displacement would be insignificant. Further, since the pointing error has a Gaussion distribution (reference 20), the 99.99% confidence limits on beam displacement for the above conditions would be 37 meters, again a relatively insignificant displacement. Since the transmitter size and number of subarrays are fixed by other conditions (references 5-8), one concludes that beam pointing errors in an MPTS would be insignificant provided the transmitter rms phase error is less than 10^{o}.

CONCLUSIONS

Closed form relations can be developed which allow quick determination of statistics of key parameters of space-to-earth microwave power transmission systems. Relations are provided for the mean power pattern at the receiver, the variance of this pattern and variance of the beam pointing. For 10^{o} rms phase error and 10% amplitude error on the transmitter the peak power density at the receiver would be degraded by only 3%. For the same conditions, the first sidelobe level is within 1.5 db of the zero error pattern with a confidence of 99.99%. The rms pointing error would be no more than 10 meters and the peak displacement would be less than 37 meters with a confidence of 99.99%.

The retrodirective phase control system is expected to perform well with a 1 km diameter transmitter providing virtually coherent radiation patterns given that the total rms insertion phase errors in the electronic modules does not exceed 10^{o} and that the spectral width of the reference does not exceed ~3,000 Hz.

REFERENCES

1. Dickinson, R. M.; and Brown, William C.: Radiated Microwave Power Transmission System Efficiency Measurements. (JPL-TM-33-727, California Institute of Technology; NAS7-100.) NASA CR-142986, 1975.
2. Dickinson, R. M.: Evaluation of a Microwave High-Power Reception-Conversion Array for Wireless Power Transmission. (JPL-TM-33-741, California Institute of Technology; NAS7-100.) NASA CR-145625, 1975.
3. Glaser, Peter E.; et al.: Feasibility Study of a Satellite Solar Power Station. NASA CR-2357, 1974.
4. Okress, Ernest C., ed.: Microwave Power Engineering. Vol. 1. Academic Press, 1968, pp. 241-269.
5. Ehricke, Krafft: Power Relay Satellite, A Means of Global Transmission Through Space. Rep. E74-3-1, Rockwell International Corp., 1974.
6. Maynard, O. E.; et al.: Microwave Power Transmission System Studies. Volume I - Executive Summary. (ER75-4368, Vol. I, Raytheon Co.; NAS3-17835.) NASA CR-134886, Vol. I, 1975.
7. Maynard, O. E.; et al.: Microwave Power Transmission System Studies. Volume II - Introduction, Organization, Environmental and Space-born Systems Analyses. (ER75-4368, Vol. II, Raytheon Co.; NAS3-17835.) NASA CR-134889, Vol. II, 1975.
8. Maynard, O. E.; et al.: Microwave Power Transmission System Studies. Volume III - Mechanical Systems and Flight Operations. (ER75-4368, Vol. III, Raytheon Co.; NAS3-17835.) NASA CR-134889, Vol. III, 1975.

9. Stevens, Grady H.; and Schuh, Richard: Space-to-Earth Power Transmission System. NASA TM X-73489, 1976.

10. Skolnik, M. I. and King, D. O.: Self-Phasing Array Antennas, IEEE Trans. Antennas Propag., Vol. AP-12, no. 2, Mar. 1964, pp. 142-149.

11. Sichelstiel, B. A.; Waters, W. M.; and Wild, T. A.: Self-Focusing Array Research Model. IEEE Trans. Antennas Propag., vol. AP-12, no. 2, Mar. 1964, pp. 150-154.

12. Pon, Chuck Y.: Retrodirective Array Using the Heterodyne Techinque. IEE Trans. Antennas Propag., vol. AP-12, no. 2, Mar. 1964, pp. 176-180.

13. Roger, Robert S.; et al.: A Supersynthesis Radio Telescope for Neutral Hydrogen Spectroscopy at the Dominion Radio Astro-Physical Observatory. Proc. IEEE, vol. 61, no. 9, Sept. 1973, pp. 1270-1276.

14. Project Cyclops - A Design Study of a System for Detecting Extraterrestrial Intelligent Life. NASA CR-114445, 1973.

15. Shore, Robert A.: Partially Coherent Diffraction by a Circular Aperture. Electromagnetic Theory and Antennas, Proceedings of a Symposium Held at Copenhagen, Denmark, June 1962, E. C. Jordan, ed., Pergamon Press, 1963, pp. 787-795.

16. Ruze, John: Antenna Tolerance Theory - A Review. Proc. IEEE, vol. 54, no. 4, Apr. 1966, pp. 633-640.

17. Schanda, E.: The Effect of Random Amplitude and Phase Errors of Continuous Apertures. IEEE Trans. Antennas Propag., vol. AP-15, no. 3, May 1967, pp. 471-473.

18. Ruze, John: Physical Limitations on Antennas. Ph. D. Thesis, MIT, 1952. (See also MIT-TR-248, AD-62351.)

19. Leichter, M.: Beam Pointing Errors of Long Line Sources. IRE Trans. Antennas Propag., vol. AP-8, no.3, May 1960, pp. 268-275.

20. Rodinelli, L. A.: Effects of Random Errors on the Performance of Antenna Arrays of Many Elements. 1959 IRE Nat. Conv. Rec., pt. 1, pp. 174-189.

21. Carver, Keith R.; Cooper, W. K.; Stutzman, Warren L.: Beam-Pointing Errors of Planar-Phased Arrays. IEEE Trans. Antenna Propag., vol. AP-12, no. 2, Mar. 1973, pp. 199-202.

22. Sherman, John W., III: Properties of Focused Apertures in the Fresnel Region. IRE Trans. Antenna Propag., vol. AP-10, no. 4, July 1962, pp. 299-408.

23. Whalen, Anthony D.: Detection of Signals in Noise. Academic Press, 1971, pp. 103-108.

APPENDIX I

Amplitude Statistics of the Receiver Pattern.

A fundamental equation defining the far field prooduced by a steady state sinusoidal field distribution is:

$$U(x_o,y_o) = \frac{1}{j\lambda Z} \int_{-\infty}^{\infty}\int U(x_1,y_1)\exp\left[-j\frac{2\pi}{\lambda Z}(x_o x_1 + y_o y_1)\right] dx_1 dy_1 \quad (I\text{-}1)$$

where,

$U(x_o,y_o)$ is the field variable of interest at the receiver location (x_o,y_o)

$U(x_1,y_1)$ is the corresponding field variable at the transmitter location (x_1,y_1)

Z is the separation between antennas

λ is the wavelength of the exciting field.

With $U(x_1,y_1)$ having only one of several quantized levels across each of N subarrays then (I-1) can be rewritten

$$U(x_o,y_o) = \frac{1}{j\lambda Z} \sum_{E=1}^{N} U_e \iint_{S_e} \exp\left[-j\frac{2\pi}{\lambda Z}(x_o x_1 + y_o y_1)\right] dx_1\ dy_1 \quad (I\text{-}2)$$

where

U_e is the complex value of the field variable on the e th subarray

S_e area of e th subarray

(x_1,y_1) coordinates within $_e$th subarray.

Assuming each subaperture area, S_e, is the same, i.e.

$$S_e = S \quad \forall\ e \quad (I\text{-}3)$$

and selecting a new coordinate system such that

$$x_1 = x_e + \xi$$
$$y_1 = y_e + \eta \qquad \text{(I-4)}$$

with (x_e,y_e) the center of the e th subaperture

then (I-2) can be written

$$U(x_o,y_o) = \frac{1}{j\lambda z} \sum_{e=1}^{N} U_e \iint_S \exp\left[-j\frac{2\pi}{z}\left\{x_o(x_e+\xi)+y_o(y_e+\eta)\right\}\right] d\xi d\eta \qquad \text{(I-5)}$$

Since (x_e,y_e) do not affect the integration in (I-5)

$$U(x_o,y_o) = \frac{1}{j\lambda z} \sum_{e=1}^{N} \left\{ U_e \cdot \iint_S \exp\left[-j\frac{2\pi}{\lambda z}(x_o\xi+y_o\eta)\right] d\xi d\eta \right\} \cdot \exp\left[-j\frac{2\pi}{\lambda z}(x_o x_e+y_o y_e)\right] \qquad \text{(I-6)}$$

Letting,

$$Fsa(x_o,y_o) = \frac{1}{j\lambda z} \iint_S \exp\left[-j\frac{2\pi}{\lambda z}(x_o\xi+y_o\eta)\right] d\xi \qquad \text{(I-7)}$$

(I-6) can be rewritten,

$$U(x_o,y_o) = Fsa \sum_{e=1}^{N} U_e \cdot \exp\left[-j\frac{2\pi}{\lambda z}(x_o x_e+y_o y_e)\right] \qquad \text{(I-8)}$$

The $U(x_o,y_o)$ is proportional to the N th order weighted sum of all the quantized levels of the transmitter field variable. The weighting factor,

$$\exp\left[-j\frac{2\pi}{\lambda z}(x_o x_e+y_o y_e)\right] \qquad \text{(I-9)}$$

accounts for the relative position or phase equivalent of each subarray.

Now (I-8) is of the same form as that analyzed by Ruze (reference 18) for a discrete array. Following Ruze's procedure we assume each subarray establishes a local value for the transmitter field variable given by,

$$U_e = \bar{U}_e \, (1+\Delta_e) \, e^{j \, \delta e} \qquad \text{(I-10)}$$

where $\bar{U}_e$ is the error free value of the field variable, Δ_e is the local error in amplitude, and δ_e is the local error in phase. Further, we assume both Δ_e and δ_e to be zero mean and having variances Δ_e^2 and δ_e^2 respectively.

Substituting (I-10) into (I-8) and calculating the power directly at the receiver,

$$\langle p(x_o,y_o) \rangle = \left| Fsa \right|^2 \cdot \sum_{em}^{N} (\bar{U}_e+\Delta U_e)(\bar{U}_m+\Delta U_m) \cdot \exp\left[-j\delta_{em}\right] \cdot \exp\left[-j \, \frac{2\pi}{\lambda \bar{z}}(x_o X_{em}+y_o Y_{em})\right] \qquad \text{(I-11)}$$

where,

$$\delta em = \delta_e - \delta_m$$

$$X_{em} = X_e - X_m$$

$$Y_{em} = Y_e - Y_m$$

$$\Delta U_e = \Delta_e \cdot \bar{U}_e$$

$$\Delta U_m = \Delta_m \cdot \bar{U}_m$$

Now $p(x_o,y_o)$ is a random variable since the amplitude errors and phase errors are random. The average or expected value of $p(x_o,y_o)$ is given by

$$\langle p(x_o,y_o)\rangle = |Fsa|^2 \cdot \sum_{em}^{N} \bar{U}_e\bar{U}_m \langle \exp(-j\delta_{em})\rangle \cdot \exp\left[-j\frac{2\pi}{\lambda z}(x_o X_{em}+y_o Y_{em})\right] \quad |Fsa|^2 \sum_{e=1}^{N} K^2\bar{U}_e^2 \qquad \text{(I-12)}$$

provided we assume ΔU_e and δ_e are statistically independent and,

$$\langle \Delta U_e^2 \rangle = K^2 \qquad \text{(I-13)}$$

Further if we use Ruze's result (reference 16),

$$\langle \exp(-j\,\delta_{em})\rangle = \begin{cases} 1 & e=m \\ \exp(-\sigma_\phi^2) & e\neq m \end{cases} \qquad \text{(I-14)}$$

then (I-12) can be written,

$$\langle p(x_o,y_o)\rangle = |Fsa|^2 \cdot \exp(-\sigma_\phi^2) \cdot \sum_{em}^{N} \bar{U}_e\bar{U}_m \cdot \exp\left[-j\frac{2\pi}{\lambda z}(x_o X_{em}-y_o Y_{em})\right] + |Fsa|^2 \cdot (1-\exp(-\sigma_\phi^2)) \cdot \sum_{e=1}^{N} \bar{U}_e^2 + |Fsa|^2 \cdot \sum_{e=1}^{N} K^2\bar{U}_e^2 \qquad \text{(I-15)}$$

Since antenna gain is defined as,

$$\text{Gain}\ (x_o,y_o) = \frac{\text{error free power density at } (x_o,y_o)}{\text{average power density at } (x_o,y_o) \text{ from isotropic radiation}} \qquad \text{(I-16)}$$

the subarrays have a gain given by,

$$Gsa = \frac{Fsa^2}{\left[\iint_S dxdy/4\pi z^2\right]} = 4\pi z^2 \frac{|Fsa|^2}{S} \qquad \text{(I-17)}$$

and the overall array has a error free gain given by

$$G(x_o,y_o)=\frac{|(Fsa)|^2 \sum_{em}^{N} \bar{U}e\bar{U}m \exp\left[-j\frac{2\pi}{\lambda z}(x_o X_{em} + y_o Y_{em})\right]}{(\bar{P}_t/4\pi z^2)} \qquad (I\text{-}18)$$

or

$$G(x_o,y_o) = \frac{4\pi z^2 |(Fsa)|^2}{\bar{P}_t} \sum_{em}^{N} \bar{U}e\bar{U}m \exp\left[-j\frac{2\pi}{\lambda z}(x_o X_{em} + y_o Y_{em})\right] \qquad (I\text{-}19)$$

where $\bar{P}_t$ is the average power contained in the error free radiation field of the transmitter and is given by

$$\bar{P}_t = \sum_{e=1}^{N} U_e^2 \cdot S \qquad (I\text{-}20)$$

Substituting (I-17), (I-19), and (I-20) into (I-15) gives the result

$$\langle p(x_o,y_o)\rangle = \frac{\bar{P}_t}{4\pi z^2}\left\{G(x_o,y_o)\exp(-\sigma_\phi^2) + \left[1 + K^2 - \exp(-\sigma_\phi^2)\right]\cdot Gsa\right\} \qquad (I\text{-}21)$$

and this is the final form of the average power density pattern presented as equation (7) in the text.

Equation (I-21) indicates the average pattern to be equivalent to the linear combination of two coherent patterns -- one produced by the overall array and one formed by a single subarray.

Since most of the RF power is confined to the pattern produced by the overall array (K, σ_ϕ small), the single subarray pattern will only affect the sidelobes.

Defining a new variable, r, such that

$$\langle r^2(x_o,y_o)\rangle = \frac{4\pi z^2 \langle p(x_o,y_o)\rangle \exp(\sigma_\phi^2)}{G(o,o)} \qquad (I\text{-}22)$$

Then substitution of (I-21) into (I-22) gives the result,

$$\langle r^2(x_o,y_o)\rangle = r_o^2\,(x_o,y_o) + E^2 \cdot \frac{Gsa}{G(0,0)} \qquad \text{(I-23)}$$

where $r(x_o,y_o)$ is the normalized magnitude of the field pattern at the receiver, r_o is the magnitude of the error free field pattern given by

$$r_o^2 = \frac{G(x_o,y_o)}{G(o,o)} \qquad \text{(I-24)}$$

and E^2 is the total mean square error given by

$$E^2 = \left[1 + K^2\text{-}\exp(-\sigma_\phi^2)\right] \cdot \exp\,(\sigma_\phi^2) \qquad \text{(I-25)}$$

Ruze has shown (reference 18) that $r(x_o,y_o)$ is statistically distributed about the error free pattern $r_o(x_o,y_o)$ in a modified Rayleigh or Rician sense i.e. of the form,

$$W\left[r(x_o,y_o)\right] = \frac{2r(x_o,y_o)}{\sigma^2} \exp\left[-\frac{\left[(r_o^2\,(x_o,y_o)+r^2(x_o,y_o)\right]}{\sigma^2}\right] I_o\left(\frac{2r_o r}{\sigma^2}\right) \qquad \text{(I-26)}$$

where I_o is the modified Bessel function of the first kind, $W\left[r(x_o,y_o)\right]$ is the probability that the normalized magnitude lies within an infinitesmal increment of $r(x_o,y_o)$, and σ^2 is the normalized variance given by

$$\sigma^2 = E^2 \cdot \frac{Gsa}{G(0,0)} \qquad \text{(I-27)}$$

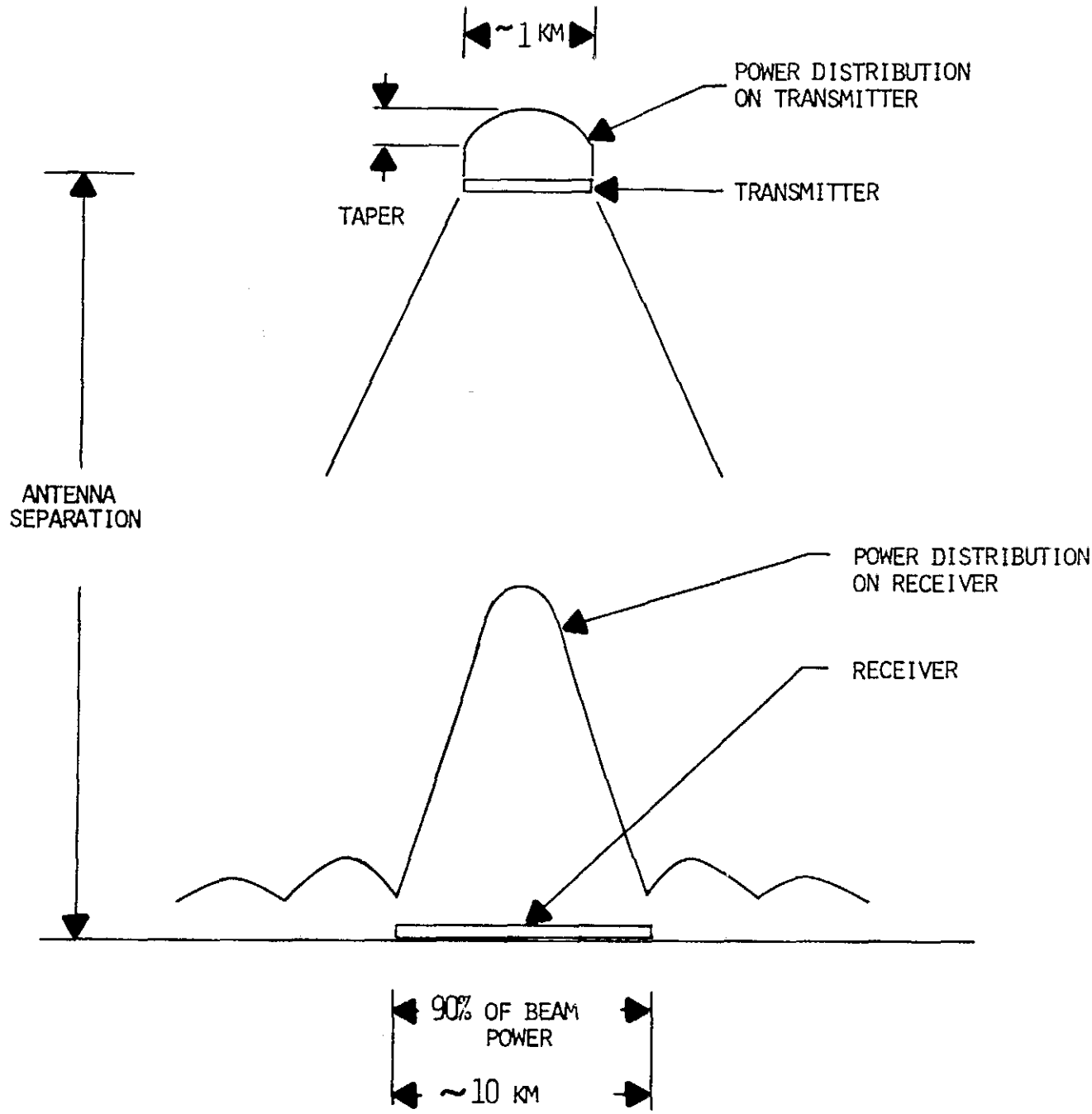

FIGURE 1 - TYPICAL GEOMETRY FOR A SPACE-TO-EARTH MICROWAVE POWER TRANSMISSION SYSTEM SHOWING A 1 KM TRANSMITTER AND A 10 KM RECEIVER WITH WHICH 90% OF THE TRANSMITTED POWER IS INTERCEPTED.

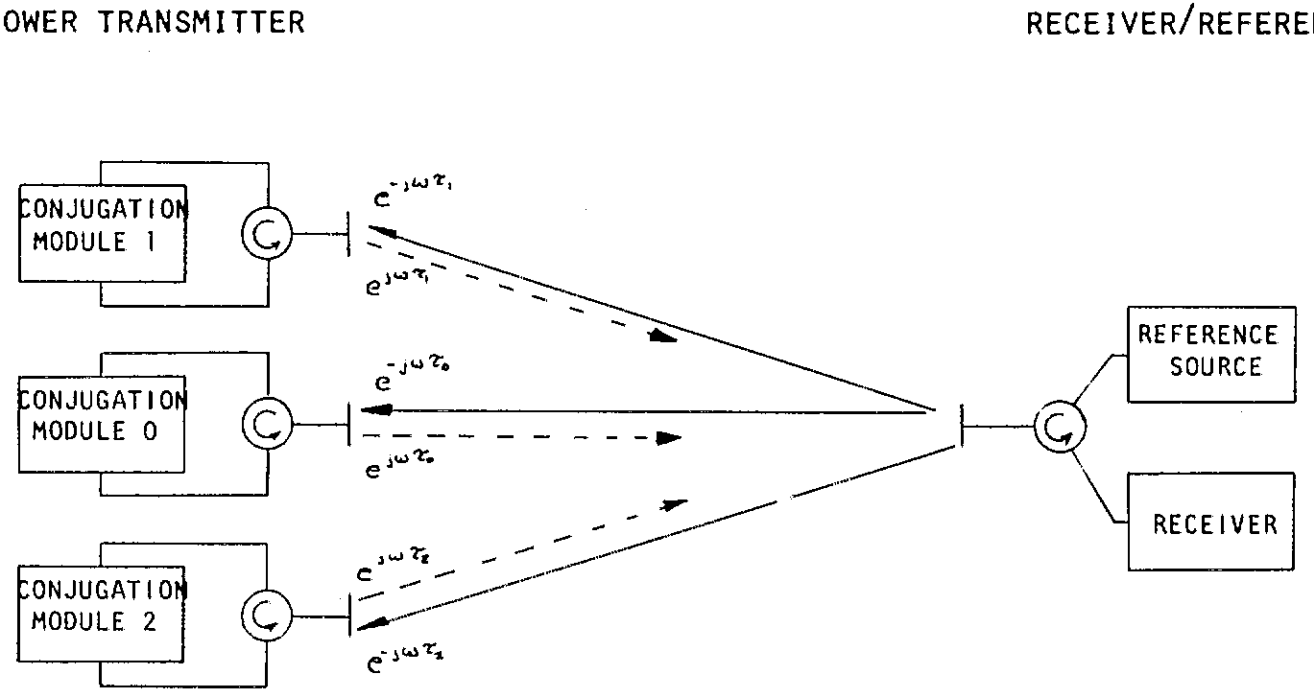

FIGURE 2 - SCHEMATIC OF TYPICAL RETRODIRECTIVE PHASE CONTROL SYSTEM SHOWING POWER TRANSMITTER CONSISTING OF SEVERAL RETRODIRECTIVE MODULES AND RECEIVER WHICH SUPPLIES THE NECESSARY PHASE REFERENCE.

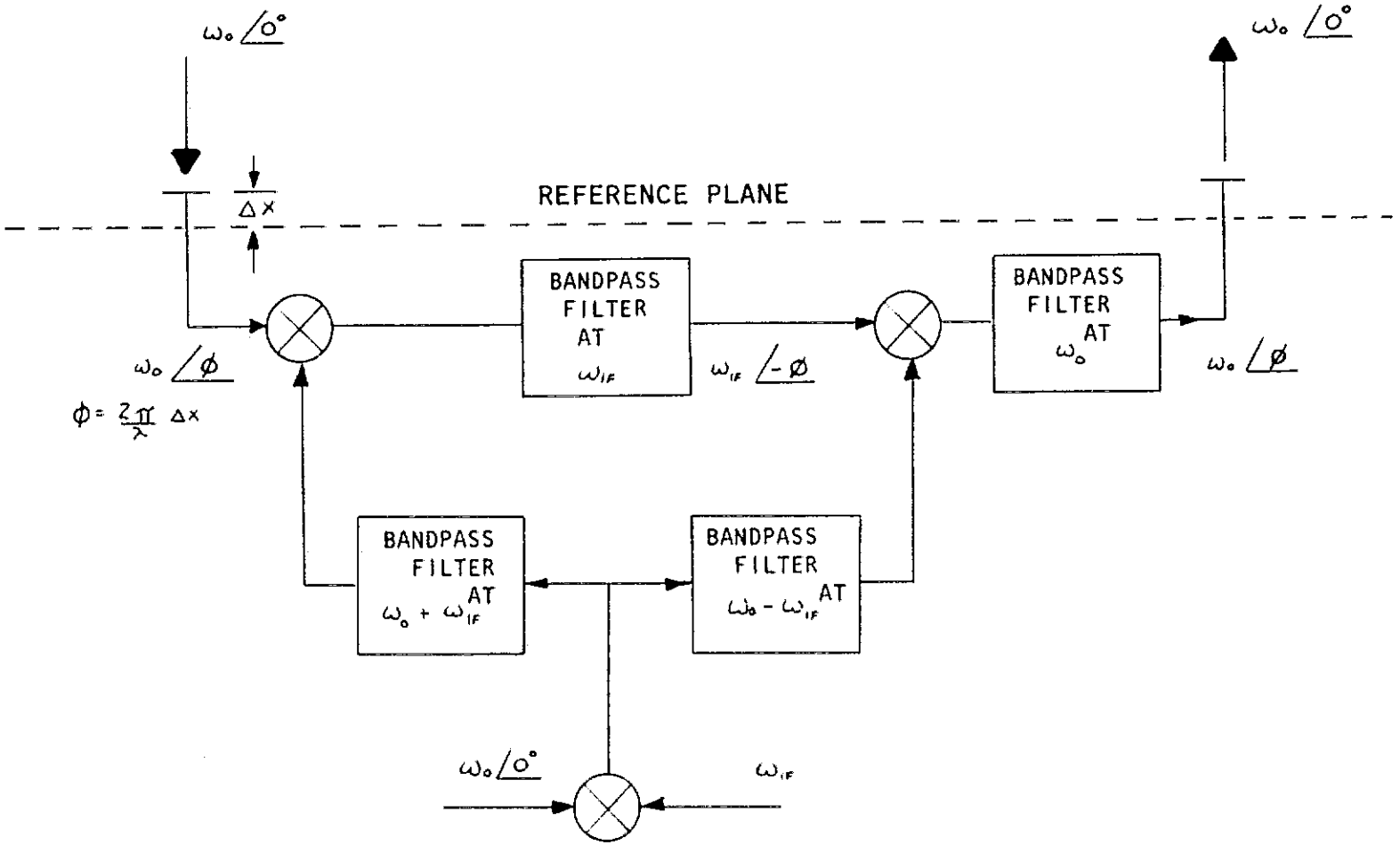

FIGURE 3 - SCHEMATIC SHOWING SCHEME FOR REALIZING REFOCUSED MICROWAVE BEAM.

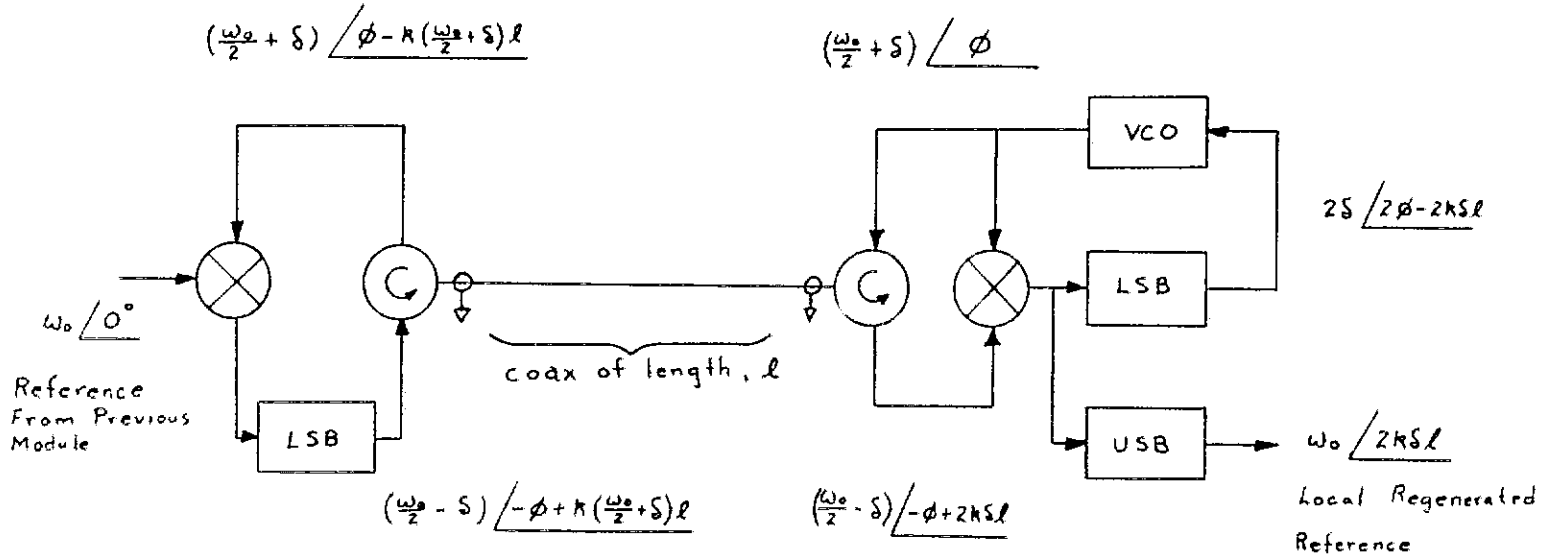

FIGURE 4 - SCHEMATIC SHOWING METHODOLOGY FOR OBTAINING ERROR-FREE DISTRIBUTION OF REFERENCE PHASE. ERROR-FREE CONDITION EXISTS WHEN PHASE LOCK LOOP (VCO-MIXER-LSB FILTER) LOCKS ONTO $\frac{W_0}{2}$ AND δ BECOMES 0.

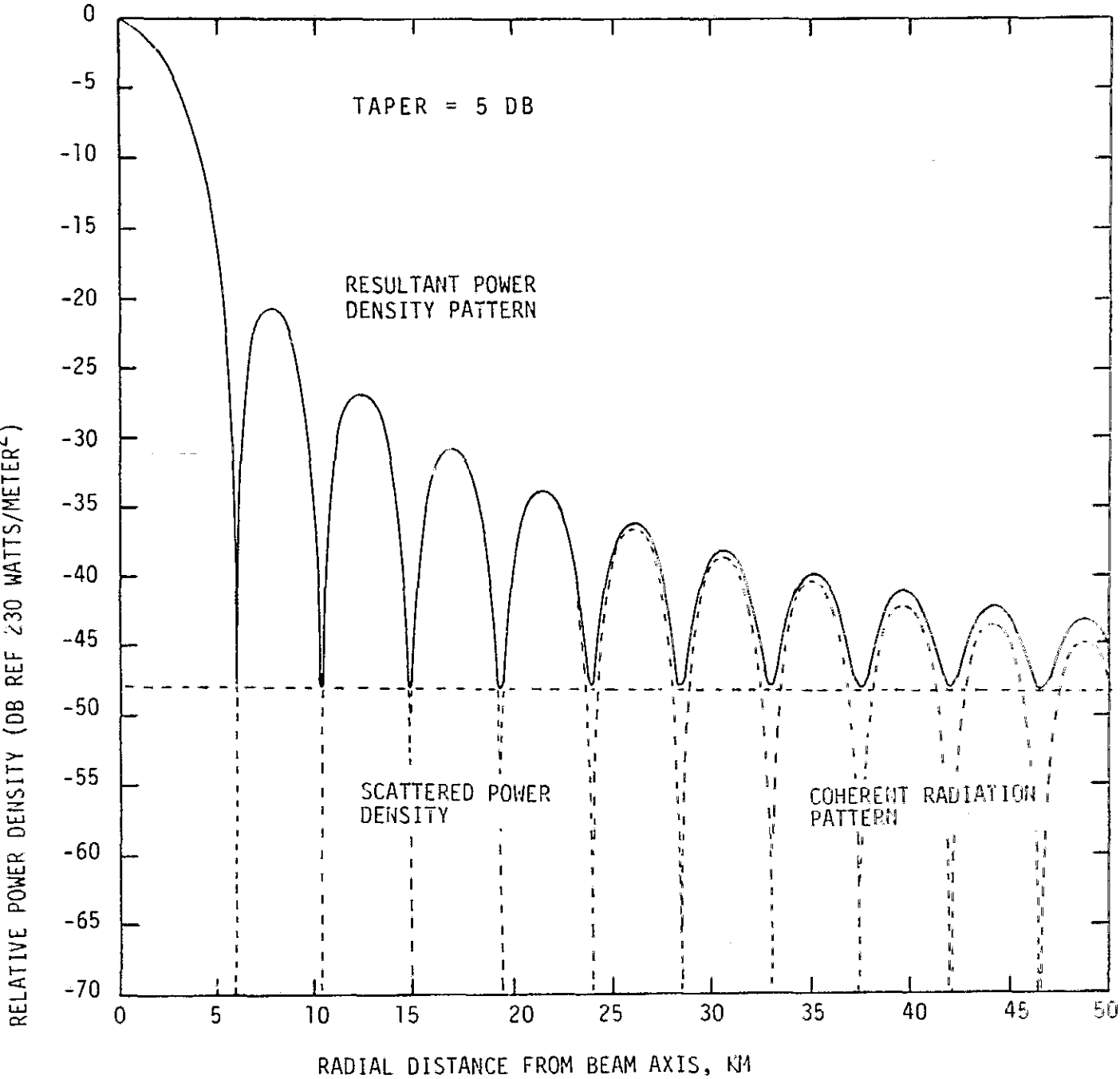

FIGURE 5 - AVERAGE COMPOSITE RECEIVER POWER DENSITY PATTERN INCLUDING EFFECTS OF RANDOM AMPLITUDE AND PHASE ERRORS.
ϕ = 10° rms, K = 0.1

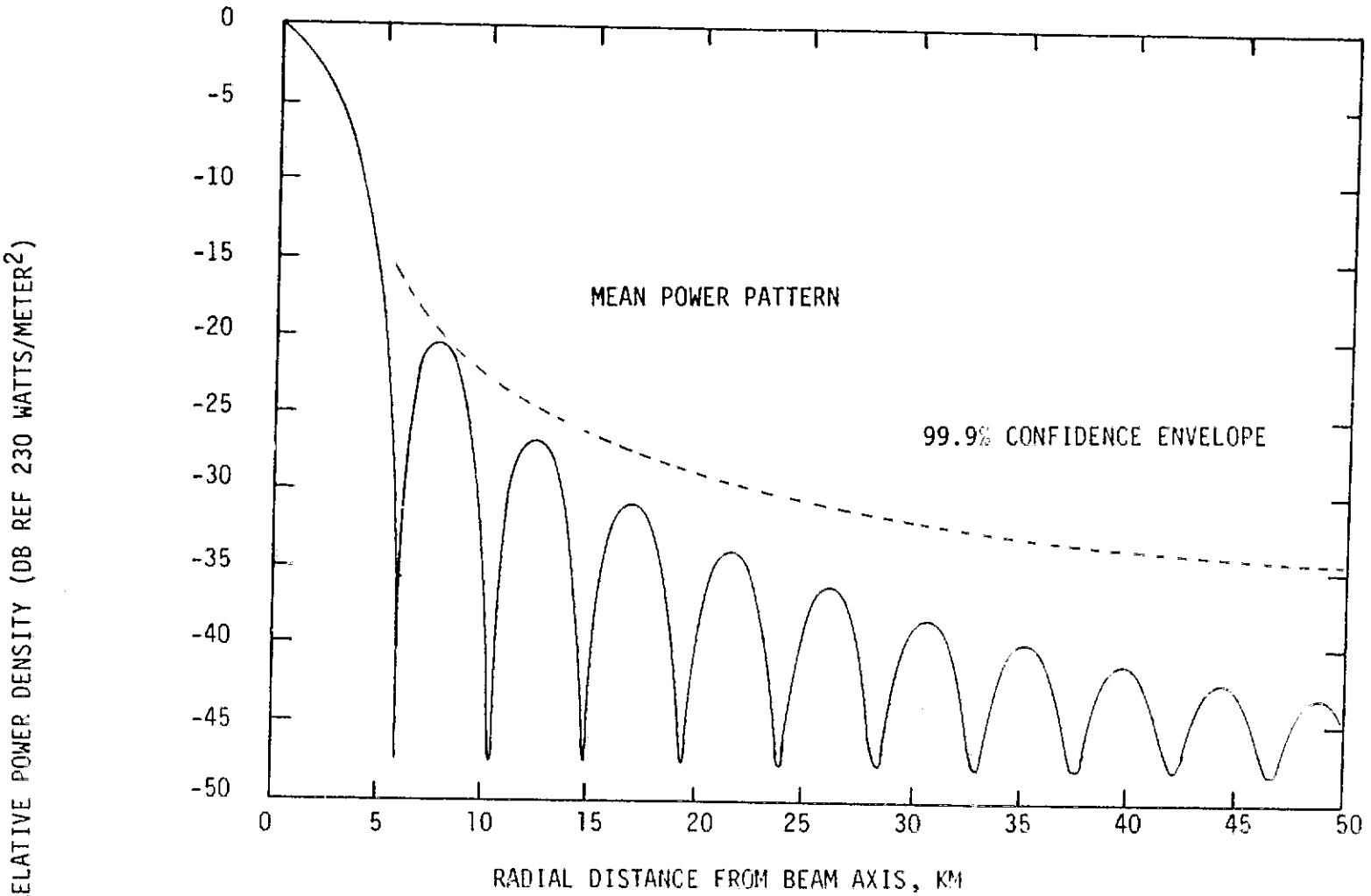

FIGURE 6 - COMPARISON OF EXPECTED ANTENNA PATTERN WITH 99.9% CONFIDENCE MAXIMUM SIDELOBE ENVELOPE